UNIVERSITY OF CANTERBURY

Construction and Testing of a Next Generation HTS Partial-Core Transformer

EEA Conference & Exhibition 2012, 22 - 20 June, Auckland

Andrew Lapthorn* [1], Pat Bodger [1]

[1] University of Canterbury
* Presenting

4/9/2012

1 INTRODUCTION

Transformers have been around for over a century and their design and construction have advanced over the years to the point where there is little room for improvement and they can be considered a mature technology. After the discovery of superconductivity in the early part of the 20th century it was thought that these new materials could be used in transformer construction. Unfortunately, due to the extremely low temperatures required for superconductivity, < 5K, expensive cryogenic technology using liquid helium was needed and the refrigeration energy required to remove any heat generated was over 1000 to 1. These factors limited the use of superconductors to dc applications such as MRI scanners and large magnets where the losses were at acceptability low levels.

In the late 1980's, a new class of superconductor was discovered which was previously thought impossible. This new type of material had critical temperatures greater than the boiling temperature of liquid nitrogen (LN_2) and became known as high temperature superconductors (HTS). These new superconductors could be cooled far more economically using liquid nitrogen and the ratio of refrigeration energy to remove heat was reduced to around 25 to 1. With the development of high temperature superconducting wire into long lengths and high current densities it became far more feasible to use this material in power frequency applications including transformers.

Many research groups around the globe have developed various high temperature superconducting transformers [1-4]. These designs have tended to be rather conventional in terms of transformer design where a standard copper winding set was replaced with a superconducting coil. One of the major advantages to using superconductors is the extremely high current density possible in the winding compared to that of conventional materials such as copper. This allows for the winding window to be much smaller than a similar rated copper transformer reducing the size and weight of the transformer.

Another way to further reduce the size and weight of a transformer is use a partial core design. This differs from the conventional transformer design because the outer limbs and connecting yokes are absent. Instead the flux return path is air. By combining the partial core concept with HTS, a new novel and compact transformer will be possible. With careful design, the performance of this type of transformer should be comparable to similar rated conventional transformers at a reduced size and weight.

2 BACKGROUND

2.1 PARTIAL CORE TRANSFORMERS

A partial core transformer (PCT) is different from a full core transformer in that the outer limbs and connecting yokes are absent from the PCT as shown in Figure 1. This enables a smaller, lighter, and easier to manufacture core as well as simplifying the overall construction of the transformer. It also means that the magnetic circuit for a PCT will consist of the core and the surrounding air. This results in a high magnetic reluctance when compared with similar rated full core transformer. Despite this, it is possible to design a PCT that performs comparably to a full core transformer under full load conditions while making significant savings on core material and transformer weight.

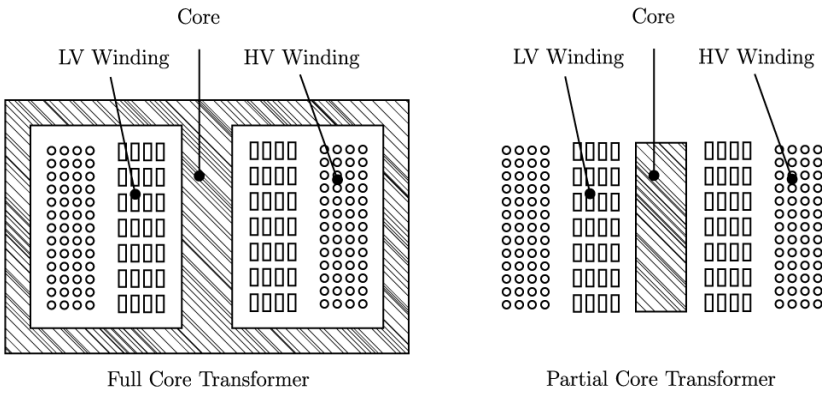

FIGURE 1: A CROSS SECTIONAL VIEW OF THE DIFFERENCES BETWEEN FULL CORE AND PARTIAL-CORE TRANSFORMERS.

A reason why there are no PCTs in the power system is because the copper losses and efficiency can be affected due to the high magnetising current, especially at low loads. The transformer can require a larger cross-section of conductor size due to the extra magnetising current, which can be 20- 30% of the load current. However, the application of HTS can eliminate this issue, i.e. very low conductor losses and small cross-sectional area, allowing for a very compact and light PCT. Furthermore, the problematic magnetising current reduces with the square of the number of turns,

$$X_m = \omega L = \frac{N^2}{\Re} \tag{1}$$

where X_m is the magnetising reactance, ω is the angular frequency equal to $2\pi f$, L is the inductance of the winding, N is the number of turns of the winding, and $\Re$ is the reluctance of the magnetic flux path. Small increases in HTS wire length and therefore number of turns, gives significant reductions in magnetising current without necessarily increases in losses. A disadvantage of the PCT is the cost of the HTS wire. However, as with other technologies, the price of HTS is likely to reduce significantly as the technology matures.

2.2 HIGH TEMPERATURE SUPERCONDUCTORS

Superconductivity is a phenomenon of exactly zero electrical resistance and expulsion of magnetic fields occurring in certain materials when cooled below a characteristic critical temperature, T_C. Zero resistance implies that there is zero electric field across a superconductor which has current through it. While this is true for low current levels, all superconductors have a limit to the current density they can handle while still maintaining zero electric field. In addition, the transition between the normal and superconducting states is not instantaneous; it is instead a smooth, non linear increase in electric field for increasing current density. This *E-J* relationship is described well by the following power law,

$$E(J) = E_C \left(\frac{J}{J_C}\right)^n \tag{2}$$

Where E_C is the electric field criterion, usually taken as 100μV/m, and J_C is the critical current density. Different materials have different *n* values, with conventional superconductors tending to have much higher *n* values than HTS.

Current in a superconductor from an external source such as a battery is referred to as transport current. It can be shown that an applied magnetic field produces screening currents in the superconductor to oppose the applied field, (Meissner Effect). So the total current in the superconductor is a combination of these two currents. As stated above, there is a limit to the current density that can flow in a superconductor. Therefore, it follows that there must be a limit to the applied magnetic field and there must exist a critical field, H_C, beyond which the superconductor becomes normal. H_C is temperature dependent, with the critical field decreasing to zero at the critical temperature.

Therefore, in order to operate an HTS transformer safely the HTS wire must be kept below critical limits as shown in Figure 2. The further below these limits the better performing the transformer will be.

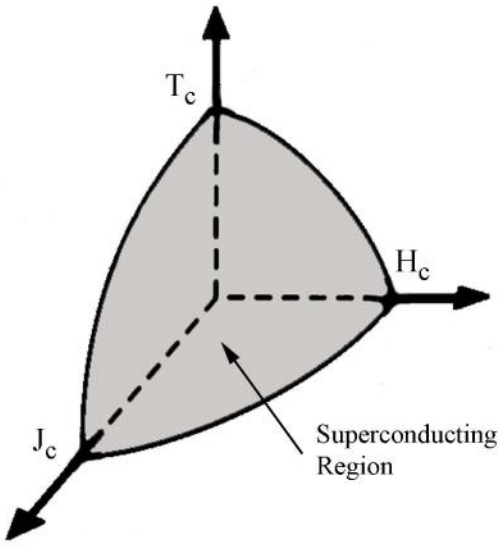

FIGURE 2: A DIAGRAM ILLUSTRATING THE CRITICAL LIMITS OF A HTS WIRE

2.3 PROTOTYPE HIGH TEMPERATURE SUPERCONDUCTING TRANSFORMERS

In 2005 the development of a 50Hz, 15kVA, 230V:115V high temperature superconductor partial core transformer (HTSPCT) was completed [5]. The transformer was designed purely as a proof of concept, rather than as a unit that would be put into service. The transformer windings were layer wound using Bi2223 HTS tape from American Superconductors. A photograph of the transformer and winding layout is shown in **Error! Reference source not found.**. The transformer failed while endurance testing under full load with the internal primary winding failing to open circuit. This prompted an investigation into the cause of failure [6]. Results from the investigation suggested the cause of failure to be insufficient cooling of the windings combined with operating too close to critical limits.

In 2009, a new experimental full core HTS transformer with an alternative winding design to enable greater cooling for the HTS wire was developed [7]. The transformer was a full core, 50Hz, 15kVA, 230V:230V two winding transformer. The design of this transformer involved the use of cooling channels allowing direct contact of the HTS wire to the liquid nitrogen coolant.

Open circuit, short circuit and loaded tests were preformed on the HTS transformer while submerged in liquid nitrogen as shown in Figure 3. Test results showed the validity of the cooling channel design concept from preventing damage to the HTS wire.

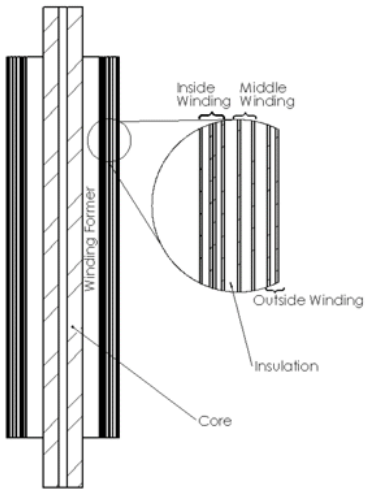

(A) DIAGRAM OF THE WINDING LAYOUT WITH RESPECT TO THE CORE, ALSO SHOWING DETAIL OF THE RELATIVE LAYER SPACING

(B) PHOTOGRAPH OF THE ORIGINAL HTSPCT

FIGURE 4: THE ORIGINAL HTSPCT

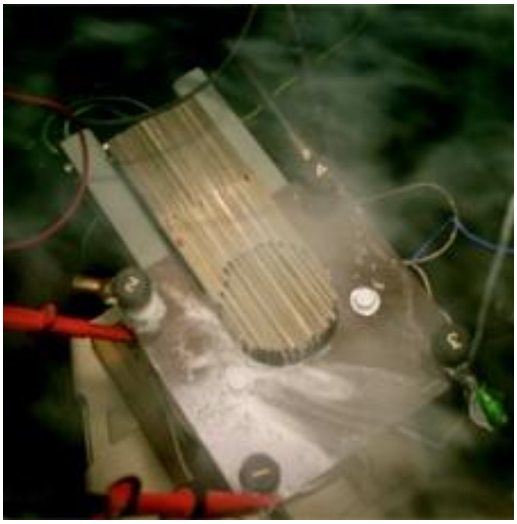

FIGURE 3: PHOTOGRAPH OF THE FULL CORE HTS TRANSFORMER BEING TESTED UNDER LIQUID NITROGEN

3 DESIGN AND CONSTRUCTION

The design and construction of a new HTSPCT was based upon the original HTSPCT which failed under high load [6]. Despite the transformer failure, there were a number of aspects of the original design that were successful. For example, the vacuum Dewar, the main assembly, the copper lead-out design, and the electrical performance prior to failure all performed to specification.

The core was designed as a parallel stacked circular core, 347 laminations of 0.23 mm, high permeability, grain orientated silicon steel. The core was bound with Vidatape S, a woven high shrink polyester tape, and hot dipped twice in an electrical baking varnish. A hole in the center of the core allows for a 1240mm long G10 fibreglass 5/8 UNC threaded rod to allow for correct positioning of the core relative to the HTS windings. The core was cut into 8 sections for experiments into the heat distribution of the core during operation.

The windings were wound with first generation HTS wire from Zenergy Power GmbH. This tape is a Bismuth based superconductor, $Bi_2Sr_2Ca_2Cu_3O_{10}$ (Bi2223), in which many superconducting filaments are encased in a silver alloy matrix using a powder-in-tube process. The manufacturers wire specification of the critical current at 77K is 136.7A in a self field. However, the alternating

magnetic fields present in the transformer result in a reduction in critical current [8], [9]. For this reason the "rated" current for the windings was set to 65A rms. The HTS wire was insulated from turn to turn short circuits by the HTS manufacturer with a spiral wrap of an electrical-grade stretched polymer foil [10]. The design specifications of the transformer are given in Table I.

TABLE I DESIGN SPECIFICATIONS OF THE HTSPCT

Core	
Parameter	**Value**
Length	470 mm
Inside Diameter	16.4 mm
Outside Diameter	80 mm
Lamination Thickness	0.23 mm
Number of Laminations	347
Inside Winding	
Parameter	**Value**
Voltage Rating	230 V
Current Rating	65 A
Winding Length	338 mm
Wire Radial Thickness	0.305 mm
Wire Axial Width	4.1 mm
Number of Layers	4
Total Turns	320
Former Diameter	115 mm
Outside Winding	
Parameter	**Value**
Voltage Rating	230 V
Current Rating	65 A
Winding Length	338 mm
Wire Radial Thickness	0.305 mm
Wire Axial Width	4.1 mm
Number of Layers	4
Total Turns	320

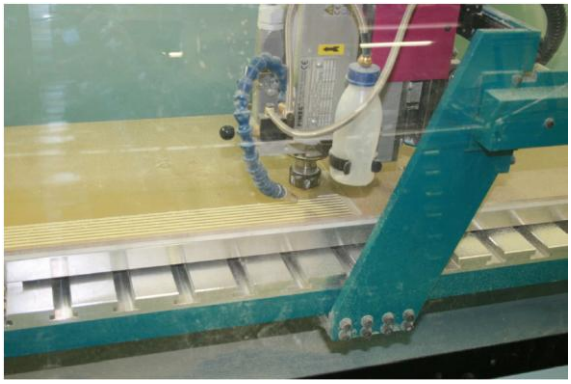

FIGURE 5: PHOTOGRAPH OF THE CAM MACHINE CUTTING THE INTER-LAYER INSULATION.

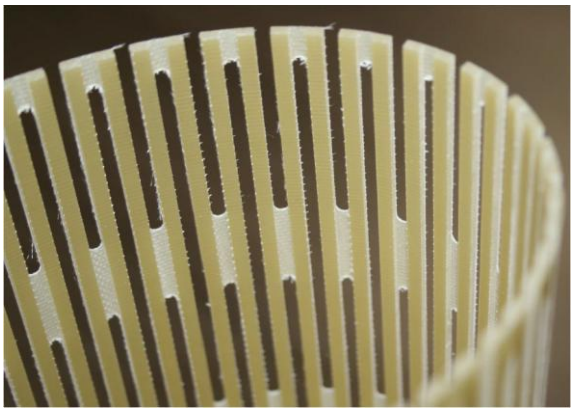

FIGURE 6: PHOTOGRAPH OF THE NEW INTER-LAYER INSULATION DESIGN.

3.1 INSULATION DESIGN

One of the most significant contributing factors of the original HTSPCT's failure was the inter-layer insulation design. The windings were bound in several layers of NOMEX® insulation paper. This prevented heat generated from the HTS conductor from being cooled sufficiently by the LN_2.

The new HTSPCT presented in this paper uses an alternative winding insulation design consisting of sheets of G10 fibreglass, 2mm thick. The sheets had 3mm wide vertical channels machined into the material every 3mm, using a CAM machine as shown in Figure 5. The depth of the cuts were 1.5mm, leaving 0.5mm of fiber sheet. In addition to this, 85mm long slots were cut into the vertical channels with slots on adjacent channels offset. The result of this machining left the fibreglass very flexible in the horizontal direction while still retaining strength as shown in Figure 6, freely allowing the flow of LN_2 around the HTS wire, and any nitrogen gas bubbles that form to escape.

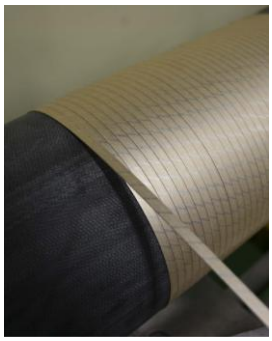

(A) The First Layer Being Wound Directly onto the Former.

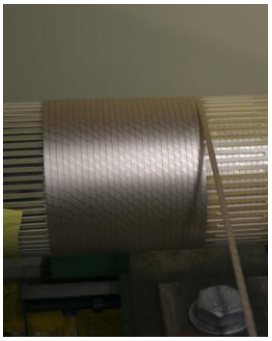

(A) The Second Layer Being Wound, Showing the Inter-layer Insulation.

(A) The Compression Connection Used to Connect the Copper Lead-outs to the Bushing Busbars.

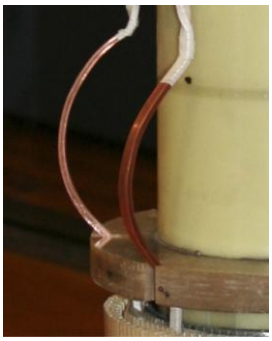

(B) Bends in the Copper Lead-outs to Allow for Thermal Expansion and Contraction.

(C) The Force Gauge Used to Measure the Wire Tension.

(D) Photograph of the Finished Winding.

Figure 7: Photographs of the Winding Process for the HTSPCT.

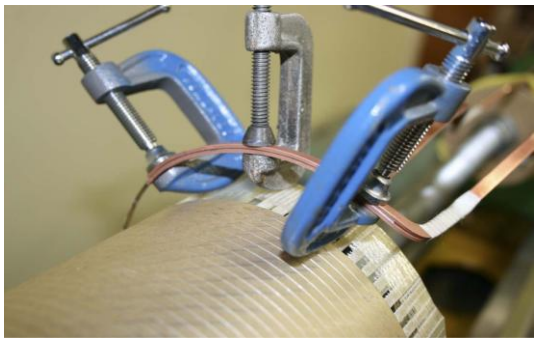

(C) One of the Copper Lead-outs About to be Soldered to the HTS Wire.

Figure 8: Details of the Copper Lead-outs Connecting the Transformer Bushings to the HTS Windings.

3.2 Transformer Construction

The windings were layer wound onto a fibreglass former that was 115mm in diameter and 402mm long. The former was made to slide over the warm bore tank and was held in place with a clamping ring also made of fibreglass. The purpose of this arrangement was to allow for the removal of the windings so that other winding arrangements could be tested, including a proposed fault current limiter (FCL), and a 2G YBCO winding. The first layer was wound directly onto the fiber former as shown in Figure 7(A), followed by a layer of the inter-layer insulation material which is held in place by the next layer of HTS wire as shown in Figure 7(B). The wire tension was controlled using a spring system and measured to ensure the wire tension remained below 15N as shown in Figure 7(C), as too much strain can cause damage to the superconductor. The final layer was wrapped in fibre reinforced tape to hold the windings in place as shown in Figure 7(D).

Copper lead-outs were used to connect the HTS windings to the transformer bushings as shown in Fig. 10. The leadouts consisted of two 1.5mm × 5mm copper conductors and were positioned radially around the transformer. The lead-outs were connected to the bushing busbars using a compression joint as shown in Figure 8(A), which was located above the LN_2 level. The bends in the lower section of the lead-outs photographed in Figure 8(B) were present to allow for thermal

expansion and contraction of the copper without pulling or pushing on the HTS windings. The copper lead-outs were soldered to the HTS wire using Indium based solder, (97% *In* 3% *Ag*), and Ersin Red Jelly flux paste. The joint was made by sandwiching approximately 10 cm of HTS wire between two specially formed copper lead-outs soldered with a temperature limited soldering iron as shown in Figure 8(C). Too high a temperature during this process can result in the HTS wire delaminating; the soldering temperature was limited to 160°C using a variac to control the soldering iron voltage.

4 TESTING AND RESULTS

4.1 KEY PERFORMANCE INDICATORS

The key performance indicators of a power transformer are the efficiency of power transfer, the voltage ratio and regulation, and the distribution of losses. Also of importance in a partial core transformer are the magnetising characteristics. These factors can be found by conducting a series of electrical tests on the transformer. The tests for traditional power transformers are outlined in the IEC 60076 series of standards. While not strictly applicable to superconducting transformers, the IEC standard can act as a guide in conducting the relevant tests.

The tests include an open circuit test, a short circuit test and a load test. Measurements of the inside and outside winding's voltage and current were taken using calibrated Fluke 41B Power Meters. The measurements were taken every 10 seconds throughout the open circuit, short circuit, and resistive load tests. The measured results were compared to calculated results from modelling found in [11]. A summary of the measured results from the tests are given in Table II.

A. Open Circuit Test Results

There is good agreement between the measured and calculated results with the largest difference being in the excitation current. The error in the current causes a similar error in the volt-amperes calculation as this is proportional to the current. The other calculated results are very close to the measured values. Figure 9 compares the calculated losses with those measured for the open circuit test. The model shows good agreement with the measured data.

Figure 10 is a plot of the open circuit voltage against the excitation current. This is a typical result for a PCT, and shows a linear increase in excitation current with applied voltage. The result also indicates that magnetic saturation of the core is not occurring in the HTSPCT. The onset of core saturation would be seen as a "flattening out" of the open circuit voltage/current relationship.

B. Short Circuit Test Results

There is good agreement between the measured and calculated results. The biggest percentage error is in the power factor with 20% error, although this result is misleading, as the power factor is very small in both cases and the actual error is small. There is also a difference between the ratio of currents and the reciprocal of the turns ratio. Once again this is because of the magnetising current component adding to the primary winding current. Figure 11 is a plot of the measured losses of the short circuit test compared to those calculated with the model. The model shows good agreement with the measured data.

TABLE II: ELECTRICAL TEST MEASUREMENTS

Open Circuit Test		
Parameter	**Measured**	**Calculated**
Inside winding voltage (V)	230.4	230
Outside winding voltage (V)	225.9	225.7
Excitation current (A)	19.4	17.6
Excitation current's phase (deg)	-87.9	-87.6
Volt-amperes (kVA)	4.5	4.054
Real power (W)	160	167
Power factor	0.04	0.04
Short Circuit Test		
Parameter	**Measured**	**Calculated**
Inside winding voltage (V)	21.1	21.1
Inside winding current (A)	66.9	67.2
Inside winding current's phase (deg)	-88	-87.5
Outside winding current (A)	66.1	66.8
Volt-amperes (kVA)	1.4	1.417
Real power (W)	65	61
Power factor	0.05	0.04
Load Test		
Parameter	**Measured**	**Calculated**
Inside winding voltage (V)	230	230
Inside winding current (A)	68.5	67.7
Inside winding current's phase (deg)	-22	-20
Outside winding voltage (V)	223	222.7
Outside winding current (A)	64.5	64.4
Outside winding current's phase (deg)	0	0
Volt-amperes (kVA)	15.7	15.562
Real power (kW)	14.7	14.625
Power factor	0.93	0.94
Load Power (kW)	14.4	14.349
Efficiency (%)	98.2	98.1
Voltage regulation (%)	2.86	3.27

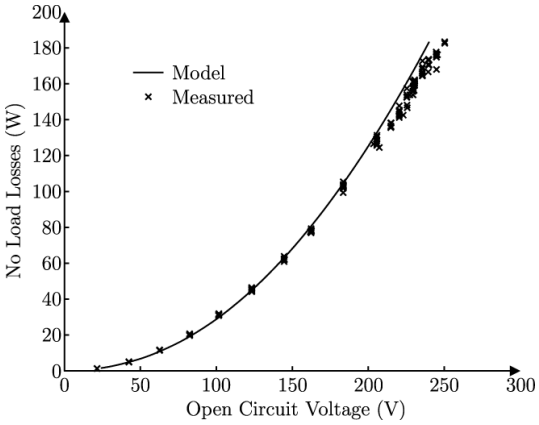

FIGURE 9: COMPARISON BETWEEN THE MEASURED AND MODELLED OPEN CIRCUIT POWER LOSS.

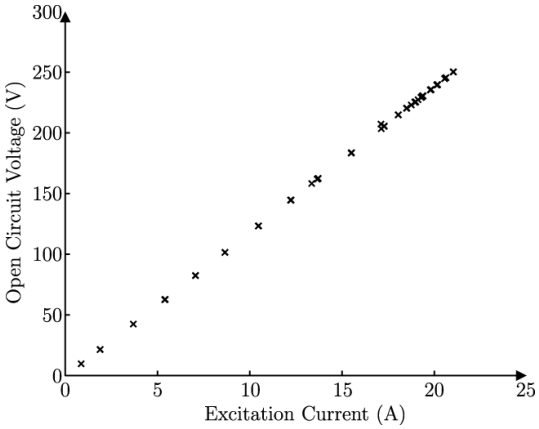

FIGURE 10: OPEN CIRCUIT VOLTAGE AGAINST EXCITATION CURRENT.

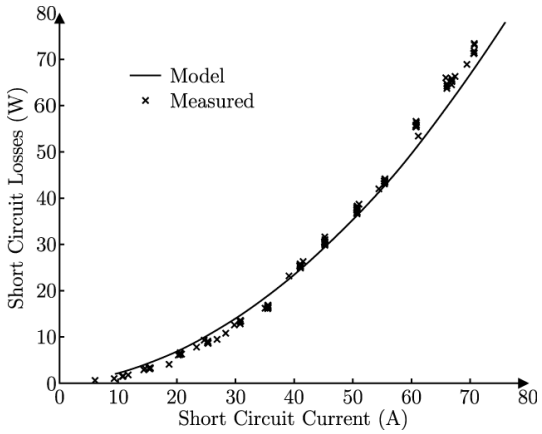

FIGURE 11: COMPARISON BETWEEN THE MEASURED AND MODELLED SHORT CIRCUIT POWER LOSS.

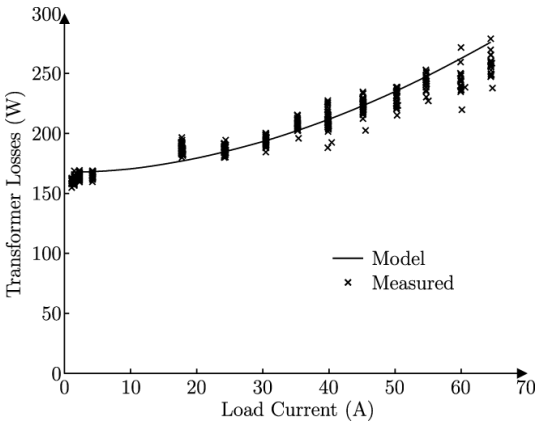

FIGURE 12: COMPARISON BETWEEN THE MEASURED AND MODELLED RESISTIVE LOAD TEST POWER LOSS.

C. Resistive Load Test Results

The resistive load test was performed with the outside winding connected to the adjustable resistive load and the inside winding connected to the single phase voltage supply. The supply was brought up to rated voltage, and measurements of the primary voltage and current were

taken as the load resistance was varied. The test was performed over several hours with the load varied from a light load up to just above the full transformer rating.

There is good agreement between the measured and calculated results with the largest errors occurring in the primary current's phase and the voltage regulation calculation. Both these errors can be attributed to the error in the magnetising current from the open circuit test. The difference in magnetising current is directly related to magnetising reactance, X_m, which has been calculated to be slightly higher than that measured. The higher magnetising current results in the primary current lagging the voltage more, as seen in the results. In addition, the difference in voltage regulation is related to the difference in no load voltage, which is again caused by the magnetising current.

Figure 12 compares the measured losses from the resistive load testing with those calculated with the model. The model shows good agreement with the measured data.

4.2 Other Experimental Data

Several other tests were conducted on the HTSPCT in addition to those mentioned above. Some of the tests, such as the insulation and dc resistance tests, were performed on the HTSPCT before those of Section 4.1 as they insure the device is electrically safe to energise. Some of the other tests, like the fault ride through test, were performed later as they were considered potentially damaging to the transformer.

D. Insulation Resistance and DC Resistance Tests

The first test performed on the HTSPCT was an insulation resistance (IR) test. This was performed with a S1-5005 insulation tester from Megger. The insulation was tested between the inside and outside windings from the bushings both prior to and after filling the LN_2 chamber. Because the main transformer assembly was made from g10 fibre, IR tests were not performed between the windings and the tank. The test voltage was 500V for 60 seconds. The results from the IR testing were 128G for the dry test and 9.1G for the wet test.

The second test performed was a dc resistance test for each winding using a MPK254 Digital Micro-Ohmmeter from Megabras. This test was performed both prior to and after filling the LN_2 chamber. Measurements were taken from between the winding's bushings. The results for the dry test were 4.133Ω and 4.741Ω for the inside and outside windings respectively. The dc resistance under LN_2 was measured as 2.3mΩ for the inside winding and 2.5mΩ for the outside winding. This result indicates that the HTS wire was superconducting and that the combined resistance of the copper lead-outs, busbars, and bushings was small.

E. Overload Test Results

The transformer was tested for an extended period of time with a 1.1 per unit loading. The original purpose of the test was to perform a high load endurance test of the transformer. However, the losses at this operating point causing LN_2 boil off were such that the test could only be run for 9 hours. Cooling of the windings during the test was from a continuous-flow type cryostat system, where the LN_2 level was maintained using a cooling system fed from a 160L LN_2 Dewar. Approximately half of the LN_2 was used to fill the HTSPCT Dewar for the test, the rest was consumed during the testing of the transformer through mechanical and electrical losses.

The transformer performance was stable throughout the testing and it is believed that with an adequate cooling system, the transformer could run continuously at this load level. A summary of the results for the overload test are given in Table III.

TABLE III: OVERLOAD TEST MEASURMENTS

Parameter	Measured
Test duration (hours)	9
Inside winding voltage (V)	231
Inside winding current (A)	71.5
Inside winding current's phase (deg)	-22
Outside winding voltage (V)	224
Outside winding current (A)	67.5
Outside winding current's phase (deg)	0
Volt-amperes (kVA)	16.5
Real power (kW)	15.4
Power factor	0.93
Load Power (kW)	15.1
Efficiency (%)	98.1
Voltage regulation (%)	2.86

These results given in Table III are comparable to those from the resistive load test of Table II The current, volt-amperes and real powers have all consistently increased in the overload test from the resistive load test, while the voltages and phase angles have remained constant.

F. Separate Source AC Withstand Voltage Test

This test was performed in accordance with IEC 60076-3. The secondary side of the HTSPCT was tied to earth and the primary winding connected to the test voltage. The test voltage was 3029V and the test duration was 60 seconds. The test voltage was supplied from a 230V to 11 kV distribution transformer fed from a variable ac source, and the test frequency was 50Hz.

Although not necessary for this test, the high voltage current was not able to be measured due to the very low capacitance of the HTSPCT insulation. The low voltage side current was measured instead and converted to the high voltage current via the distribution transformer turns ratio.

The low voltage current was measured at 109mA which converted to 2.27mA on the high voltage side. This gives an estimated insulation capacitance of 2.4 nF resulting in a resonant frequency of approximately 16 kHz.

G. Fault Ride Through

The final test performed on the HTSPCT was a fault ride through test. This test was performed last as it was considered to have the highest potential for transformer failure. In this test, the HTSPCT secondary winding was connected to the 15 kW resistive. The rated voltage was applied to the primary winding through a 600A supply. The secondary winding was then short circuited via a manually operated switch. The voltage and current for the primary and secondary windings was monitored with a four channel oscilloscope. The measured fault level was approximately 350A rms. This lasted for about 7 cycles before circuit breaker was operated.

Oscilloscope traces of the primary voltage and current for one particular measurement are shown in Figure 13. From the trace, it is apparent that the inception of the fault occurred approximately 0.01 seconds before the oscilloscope triggered at time equal to 0 seconds. A slight reduction in the voltage magnitude as the fault current appears is apparent, which is due to the voltage drop across the impedance of the supply. The transient nature of the waveform is entirely dependent on the point of the wave where the fault occurs.

Figure 12 shows the measured voltage and current of the secondary winding for the same instance. At the time the fault is applied, the secondary voltage reduces to zero. The measured secondary current is very similar to that of the primary winding, with approximately the same magnitude and transient component. A visual inspection was carried out on the transformer upon completion of the testing. The transformer was allowed to return to room temperature prior to opening the tank to prevent moisture from damaging the windings. The transformer suffered no visible damage as a result of this test.

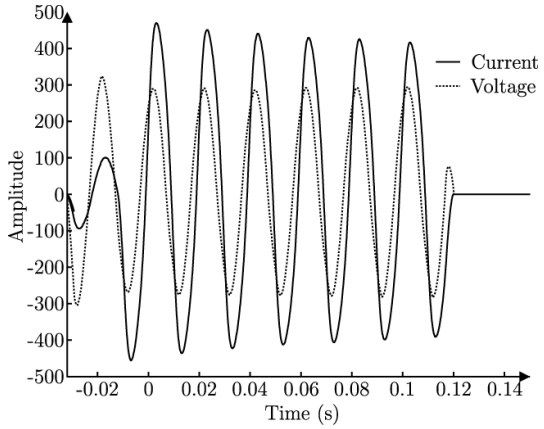

FIGURE 13: OSCILLOSCOPE TRACES OF THE PRIMARY VOLTAGE, IN VOLTS, AND CURRENT, IN AMPERES, DURING THE FAULT RIDE THROUGH TEST.

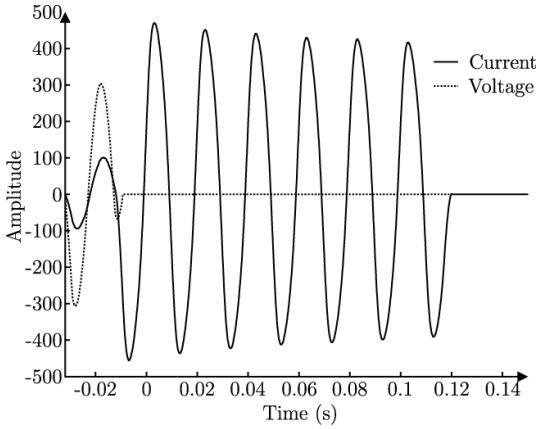

FIGURE 14: OSCILLOSCOPE TRACES OF THE SECONDARY VOLTAGE, IN VOLTS, AND CURRENT, IN AMPERES, DURING THE FAULT RIDE THROUGH TEST.

5 CONCLUSIONS

This paper has presented a new design for a 15 kVA 230V high temperature superconducting partial core transformer. The new design offers improvement over the original HTSPCT with an updated inter-layer insulation design that allows for greater contact between the LN_2 coolant and the HTS conductor. The transformer was tested over this range of operating conditions and compared with a model. There was good agreement.

6 ACKNOWLEDGMENT

The authors would like to acknowledge the support from Industrial Research Limited for the duration of this research. Their contributions of materials, scholarships, measurements on the HTS samples, and knowledge were invaluable to the completion of this project.

7 REFERENCES

[1] THEROND, P.G., LEVILLAIN, C., PICARD, J.F., BUGNON, B., ZUEGER, H., HORNFELDT, S., FOGELBERG, T., PAPST, G. AND BONMANN, D. (1998), 'High Temperature 630 kVA Superconducting Transformer', In *Cigr´e Paris Sessions*, Paris, France.

[2] SCHWENTERLY, S.W., MCCONNELL, B.W., DEMKO, J.A., FADNEK, A., HSU, J., LIST, F.A., WALKER, M.S., HAZELTON, D.W., MURRAY, F.S., RICE, J.A., TRAUTWEIN, C.M., SHI, X., FARRELL, R.A., BASCUIIAN, J., HINTZ, R.E., MEHTA, S.P., AVERSA, N., EBERT, J.A., BEDNAR, B.A., NEDER, D.J., MCILHERAN, A.A., MICHEL, P.C., NEMEC, J.J., PLEVA, E.F., SWENTON, A.C., SWETS, W., LONGSWORTH, R.C., JOHNSON, R.C., JONES, R.H., NELSON, J.K., DEGENEFF, R.C. AND SALON, S.J. (1999), 'Performance of a 1-MVA HTS Demonstration Transformer', *Applied Superconductivity, IEEE Transactions* -, Vol. 9, No. 2, pp. 680–684.

[3] PLEVA, E. AND SCHWENTERLY, S. (2004), 'Assembly and test of 5/10 MVA HTS transformer', In *Power Engineering Society General Meeting*, 2004. IEEE, June, pp. 1431–1435.

[4] KIM, S.H., KIM, W.S., CHOI, K.D., JOO, H.G., HONG, G.W., HAN, J.H., LEE, H.G., PARK, J.H., SONG, H.S. AND HAHN, S.Y. (2005), 'Characteristic Tests of a 1 MVA Single Phase HTS Transformer With Concentrically Arranged Windings', *Applied Superconductivity, IEEE Transactions* -, Vol. 15, No. 2, pp. 2214–2217.

[5] BODGER, P. S., ENRIGHT, W. G. AND HO, V. (2005), "A low voltage, mains frequency, partial core, high temperature, superconducting transformer," In *Australasian Universities Power Engineering Conference (AUPEC'05)*, Brisbane, Australia, Sep., CD

[6] LAPTHORN, A.C., CHEW, I., ENRIGHT, W.G. AND BODGER, P.S. (2011), 'HTS Transformer: Construction Details, Test Results, and Noted Failure Mechanisms', *Power Delivery, IEEE Transactions on* , Vol. 26, No. 1, pp.394-399.

[7] LAPTHORN, A.C., CHEW, I. AND BODGER, P.S. (2010), 'An Experimental High Temperature Superconducting Transformer: Design, Construction and Testing', In *Electricity Engineers' Association (EEA) Conference*, Christchurch, New Zealand, June, pp.1-9.

[8] ZHU, Q., CHEN, D. X. AND HAN, Z. H. (2004), "Field dependent critical current of Bi-2223/Ag tapes at different thermo-mechanical stages," *Superconductor Science and Technology*, vol. 17, pp. 756–763.

[9] LEGHISSA, M., FISCHER, B., ROAS, B., JENOVELIS, A., WIEZORECK, J., KAUTZ, S. AND NEUMULLER, H.-W. (2007), "Bi-2223 Multifilament Tapes and Multistrand Coniductors for HTS Power Transmission Cables," *Applied Superconductivity, IEEE Transactions* -, vol. 7, no. 2, pp. 355–358.

[10] KELLERS, J., BÄCKER, M., BÜHRER, C., MÜLLER, J., RATH, A., REMKE, S. AND WIEZORECK, J. (2005) "Flexible HTS Wires: From Start-Up of a Full- Sized Plant to Industrial Applications," *Applied Superconductivity, IEEE Transactions* -, vol. 15, no. 2, pp. 2522–2525.

[11] LAPTHORN, A.C. (2012), "High Temperature Superconducting Partial Core Transformers", *PhD thesis*, Univ. of Canterbury, Christchurch, New Zealand.